Ma, J., Fu, C., Zhu, W., Lu, K., and Yang, Y. (January 21, 2022). "Stochastic analysis of lubrication in misaligned journal bearings." ASME. J. Tribol. doi: https://doi.org/10.1115/1.4053626

Jiaojiao Ma
School of Mechatronics Engineering,
Foshan University,
Foshan 528000, China
e-mail: majiaojiao@fosu.edu.cn

Chao Fu[1]
Institute of Vibration Engineering,
Northwestern Polytechnical University,
Xi'an 710072, China
e-mail: fuchao@nwpu.edu.cn

Weidong Zhu
Department of Mechanical Engineering,
University of Maryland,
Baltimore County,
Baltimore, MD 21250
e-mail: wzhu@umbc.edu

Kuan Lu
Institute of Vibration Engineering,
Northwestern Polytechnical University,
Xi'an 710072, China
e-mail: lukuan@nwpu.edu.cn

Yongfeng Yang
Institute of Vibration Engineering,
Northwestern Polytechnical University,
Xi'an 710072, China
e-mail: yyf@nwpu.edu.cn

Stochastic Analysis of Lubrication in Misaligned Journal Bearings

Misalignment is common in hydrodynamic journal bearings and the causes of it can be diversified, making the lubrication performance exhibits stochasticity. Lubricant viscosity often heavily depends on temperature, which may vary during service and result in unexpected deviations. This article analyzes the stochastic lubrications of a cylindrical hydrodynamic journal bearing with misalignment under uncertainties. The stochastic Reynolds equation governing the misaligned journal bearing is discretized by the polynomial chaos expansion (PCE), an efficient uncertainty tracking tool, and then solved by the finite difference method to obtain sampled lubrication. The crude Monte Carlo simulation is used to verify the performance of the PCE frame. Various critical lubrication performance parameters are studied comprehensively by the ensemble mean, standard deviation, probability density function, and cumulative distribution function. Insightful inspections are provided on the stochastic results, and it is found that the misalignment and different stochastic parameters may cause significant effects on the lubrication performance. The new findings in the present study will guide the robust design and analysis of general hydrodynamic journal bearings. [DOI: 10.1115/1.4053626]

Keywords: misalignment, stochastic analysis, polynomial chaos, hydrodynamic lubrication, journal bearings, tribological systems

1 Introduction

Rotating machinery is commonly mounted on hydrodynamic journal bearings, which support the heavy loads and affect the stability of the system [1–3]. Ideally, the rotary shaft will be perfectly aligned with the bearing centerline and the oil film provides expected hydrodynamic lubrication [4,5]. However, it is recognized in practice that there is always a certain degree of misalignment between the journal and bush causing them to be unparallel [6,7]. The reasons for it vary from shaft deformation due to external load, inappropriate assembling, manufacturing error, and thermal effects. A direct effect of misalignment is the reduction of minimum oil-film thickness in the journal bearing, which is responsible for the load-carrying capacity generation and preventing the direct contact between the shaft and bearing surfaces. The lubrication performance and life expectancy of journal bearings and relevant characteristics of the rotor system will be significantly altered [8–11]. Many researchers worldwide have made enormous efforts to understand the hydrodynamic lubrication of misaligned journal bearings. Sun and Gui [12] assessed the lubrication characteristics of a journal bearing with misalignment caused by shaft deformation, including the load-carrying capacity, end leakage flowrate, and the misalignment moment. An experimental analysis was carried out by Bouyer and Fillon [13] under a variable misalignment torque, and it was found that the bearing performances were more influenced by a low rotation speed or load. He et al. [14] investigated the effects of misalignment caused by asymmetry based on a simple stepped shaft model. The turbulence involved mixed lubrication is studied for a misaligned journal bearing, and evaluations were done concerning different lubrication characteristics [15–17]. Nikolakopoulos and Papadopoulos [18] developed a mathematical model to describe the joint relationship among the friction force, the misalignment angles, and wear depth.

The inherent parametric stochasticity is barely considered, however, in most of the reported works that deal with misaligned hydrodynamic journal bearings based on deterministic physical models and working conditions [19]. Consensus has been reached in the wider community that mechanical systems are always subject to various uncertainties [20–23]. For a journal bearing working in the hydrodynamic regime, the situation is even more prominent [24–27]. The working conditions, such as temperature and load fluctuations, will change the pressure distribution of lubricants [28,29]. Other factors include the dispersion of materials, wear, and all types of errors. Moreover, the misalignment can be affected by different aspects which are difficult to accurately identify, making it behave in an uncertain manner. To capture the whole picture of misaligned journal bearings, the stochasticity in the model should be included and corresponding lubrication analysis needs to be performed. Cavalini et al. [30] modeled the uncertainties in fluid film bearings for a rotor-bearing system using fuzzy dynamic analysis. Specifically, the effects of variabilities in the bearing radial clearance and oil viscosity on the rotor orbits and unbalanced responses were analyzed. The same types of uncertainties were considered by Visnadi and Castro [31] when investigating the stability threshold of the cylindrical journal bearings. Tyminski et al. [32] employed the Bayesian inference to identify the journal bearing parameters and further evaluated the rotor responses. Koutsovasilis and Schweizer [33] used a data mining technique to reveal the influences of parameter variations in oil-film bearings. They presented a comprehensive stochastic study on various lubrication characteristics. In Ref. [34], the effects of surface roughness, as well as stochastic eccentricity ratio, were determined by using a radial basis function-based surrogate model. As can be inferred from the above literature, the efficiency for the uncertainty quantification in hydrodynamic lubrication analysis of journal bearings plays a critical role in practical implementation. It is the case because the laminar flow in journal bearings is governed by the

[1]Corresponding author.

Contributed by the Tribology Division of ASME for publication in the JOURNAL OF TRIBOLOGY. Manuscript received October 16, 2021; final manuscript received January 15, 2022; published online February 25, 2022. Assoc. Editor: Ling Wang.

Reynolds equation, which is a two-dimensional partial differential equation (PDE) and can be time-consuming when repetitively solved by numerical algorithms. The above-mentioned fact excludes the direct application of the classic Monte Carlo simulation (MCS) due to its low convergence rate and enormous computational requirement. Moreover, the way of implementation of an uncertainty analysis method matters a lot to the engineering practice, i.e., whether the method can be non-intrusively adapted to different models or situations [35]. For intrusive methods, the original solver of the deterministic system needs to be modified and the stochasticity should be considered in every deduction step, which makes the solution process difficult to understand and realized. For example, the perturbation technique dedicated to small uncertainty is intrusive and relies on analytical derivative information, which is quite demanding for complicated engineering structures. Another disadvantage is that it is hard to extend to higher-order models due to its derivation nature. However, the non-intrusive algorithms treat the deterministic problem as a black box and only a limited number of samples of interesting outputs should be drawn. It can be a great alleviation to complicated scenarios where multiple modules are involved. The PCE can serve such a role with excellent performance, and this has been evidenced by applications in various fields [36–38].

So far, the stochastic lubrication performances of journal bearings with misalignment remain unclear. The PCE, preferably utilized in a non-intrusive way, has not been generalized into uncertainty analysis of such misaligned systems. In the present study, we propose to use the PCE with the numerical algorithms to solve the stochastic Reynolds equation for misaligned journal bearing. The analysis framework operates in a non-intrusive and efficient way, which is a major advantage in engineering computation. A comprehensive hydrodynamic analysis is carried out including stochasticity in the oil viscosity (mainly caused by the temperature variation and oil degradation) and misalignment of the journal to unveil their individual and combined effects on lubrication characteristics. Furthermore, verifications of the obtained results are carried out in terms of calculation accuracy and efficiency.

The remainder of this paper is as follows. In Sec. 2, the modeling of a hydrodynamic journal bearing with misalignment is illustrated. Propagating the uncertainty into the lubrication performance based on the generalized PCE is explained in Sec. 3. Intensive stochastic investigations are provided in Sec. 4 considering two typical uncertainties. The main conclusions are given in Sec. 5.

2 Theoretical Misaligned Journal Bearing Model

Figure 1 shows the physical model of a cylindrical journal bearing with angular misalignment and its projected view. The width of the bearing is L and the geometric center of the journal is O if there is no misalignment. Points C_1, C_0, and C_2 are the intersections of the journal centerline with the front-end cross-section, mid-plane, and rear-end cross-section, respectively. The coordinates placement can be found in Fig. 1. Based on the geometry, the thickness of oil film in the bearing is defined as [12]

$$h = c + e_0(\varphi - \varphi_0) + z\tan\gamma\cos(\varphi - \alpha - \varphi_0) \tag{1}$$

where c is the nominal bearing clearance, e_0 and φ_0 represent the eccentric vector in the mid-plane, φ and z are the circumferential and axial coordinates, α is the angle between the journal centerline projection and line OC_0, and γ denotes the misalignment angle.

The governing equation of the laminar flow in journal bearings can be described as the two-dimensional Reynolds equation [39]

$$\frac{1}{R^2}\frac{\partial}{\partial\varphi}\left(h^3\frac{\partial p}{\partial\varphi}\right) + \frac{\partial}{\partial z}\left(h^3\frac{\partial p}{\partial z}\right) = 6\omega\mu\frac{\partial h}{\partial\varphi} + 12\mu\frac{\partial h}{\partial t} \tag{2}$$

where R is the radius of the bearing, p represents the pressure of lubricant, ω denotes the angular speed of the shaft, and μ is the lubricant viscosity. When the steady-state lubrication is concerned, the second term of the right-hand side of Eq. (2) is neglected.

As explained previously, the journal bearing operating in hydrodynamic regime is inherently subject to stochasticity due to a variety of reasons. Especially, the misalignment magnitude by nature is hard to accurately define or measure. When the randomness of the physical model is taken into consideration, the deterministic Reynolds equation gets modified to include the stochasticity in fluid motion; i.e., Eq. (2) will take the following form:

$$\frac{1}{R^2}\frac{\partial}{\partial\varphi}\left(h^3(\tau)\frac{\partial p(\tau)}{\partial\varphi}\right) + \frac{\partial}{\partial z}\left(h^3(\tau)\frac{\partial p(\tau)}{\partial z}\right) = 6\omega\mu(\tau)\frac{\partial h(\tau)}{\partial\varphi} \tag{3}$$

where τ designates a random factor denoting the stochasticity. In Eq. (3), the oil-film thickness is expressed with randomness which allows considering the deviation in bearing geometry properties and external load. Moreover, the viscosity is taken as stochastic into account for the uncertain lubricant property or temperature fluctuation.

3 Stochastic Analysis of Hydrodynamic Lubrication

In this section, the numerical procedure for determining the stochastic behaviors of the journal bearing is developed. The geometry of the bearing model or properties of the lubricant can be treated as stochastic variables or processes. Most of the stochastic processes in the real world cannot be modeled rigorously by the sum of multistochastic integrals of orthogonal polynomials, except for several special cases such as the Hermite–Brownian process. Alternatively, an approximation can be developed. Based on the Wiener

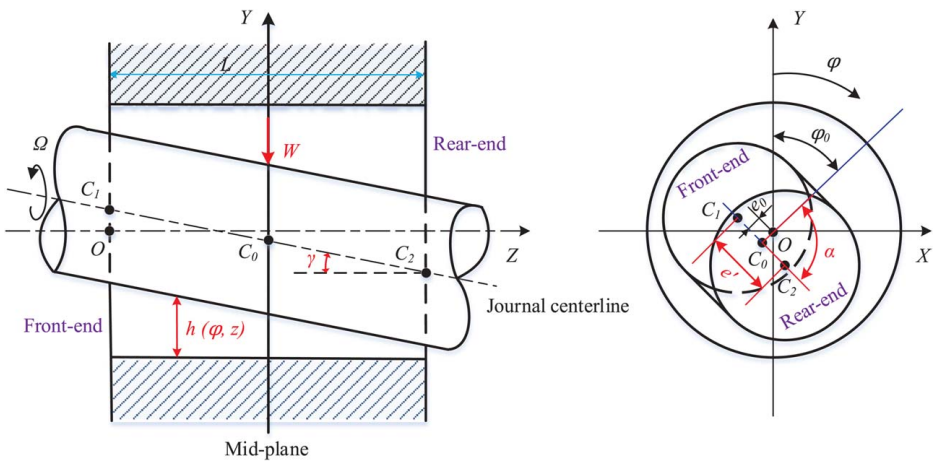

Fig. 1 Hydrodynamic journal bearing with misalignment

homogeneous chaos theory, the PCE [40–42] represents uses a set of orthogonal polynomial chaos bases of stochastic variables to approximate the random inputs and outputs. The Karhunen–Loeve expansion coupled with the Galerkin projection is often employed to find practical solutions. In such a way, the stochastic system is converted to a set of deterministic systems and the expansion coefficients can then be obtained. Further, the surrogate of the uncertain problem can be constructed, and the statistical moments of the stochastic outputs can be derived based on the explicit surrogate. There is a set of optimal orthogonal polynomials for different probabilistic distributions to achieve the best approximation of stochastic variables [40]. For example, the Legendre polynomials are optimal for uniform distribution, Laguerre polynomials give the best approximation of Gamma distribution while the Hermite polynomials should be matched with Gaussian variables. The last pair, which has been widely adopted in uncertain engineering systems, will be used in this study.

To implement the surrogate modeling based on the PCE, the uncertain parameters in the bearing (such as lubricant viscosity and misalignment angle) should be expressed as

$$\begin{cases} \mu(\tau) = \bar{\mu}(1 + \delta_1 \xi_1(\tau)) \\ \gamma(\tau) = \bar{\gamma}(1 + \delta_2 \xi_2(\tau)) \end{cases} \tag{4}$$

where $\bar{\mu}$ and $\bar{\gamma}$ are the mean of stochastic lubricant viscosity and misalignment angle, δ_1 and δ_2 are the standard deviation of them, $\xi_1(\tau)$ and $\xi_2(\tau)$ denote two standard Gaussian variables. If more random parameters in the bearing should be considered, a similar expression can be obtained as in Eq. (4). Then, a multidimensional random input array $\mathfrak{I}(\tau) = \{\mu(\tau), \gamma(\tau), \ldots\}$ and a standard random variable vector $\boldsymbol{\xi}(\tau)$ will be generated

$$\begin{cases} \mathfrak{I} = \bar{\mathfrak{I}}(1 + \boldsymbol{\delta}\boldsymbol{\xi}(\tau)) \\ \boldsymbol{\delta} = [\delta_1, \delta_2, \ \ldots, \delta_n] \\ \boldsymbol{\xi}(\tau) = [\xi_1(\tau), \xi_2(\tau), \ \ldots, \xi_n(\tau)] \end{cases} \tag{5}$$

where $\xi_i \sim N(0, 1)$, $i = 1, 2, \ \ldots, n$ and n is the number of stochastic parameters.

Denote the random steady-state characteristics of the journal bearing by $G(\mathfrak{R}, \mathfrak{I}(\tau))$, where $\mathfrak{R}$ is the non-random parameter set of the model. From Eq. (5), we know that the actual stochastic parameter vector can be projected to the standard Gaussian variable vector, and then, the latter will be used in the deduction without loss of generality. The deterministic parameter set is omitted for the sake of simplicity without confusion and then it is written as $G(\boldsymbol{\xi}(\tau))$. In a probability space Ω, the stochastic lubrication characteristics can be represented on the polynomial chaos basis by

$$\begin{aligned} G(\boldsymbol{\xi}(\tau)) &= g_0 \boldsymbol{\psi}_0 + \sum_{k_1=1}^{\infty} g_{k_1} \boldsymbol{\psi}_1(\xi_{k_1}(\tau)) + \sum_{k_1=1}^{\infty} \sum_{k_2=1}^{k_1} g_{k_1 k_2} \boldsymbol{\psi}_2(\xi_{k_1}(\tau), \xi_{k_2}(\tau)) \\ &\quad + \sum_{k_1=1}^{\infty} \sum_{k_2=1}^{k_1} \sum_{k_3=1}^{k_2} g_{k_1 k_2 k_3} \boldsymbol{\psi}_3(\xi_{k_1}(\tau), \xi_{k_2}(\tau), \xi_{k_3}(\tau)) + \cdots \\ &= \sum_{k=0}^{\infty} g_k \boldsymbol{\psi}_k(\boldsymbol{\xi}(\tau)) \end{aligned} \tag{6}$$

where g_k is the unknown polynomial chaos (PC) coefficient and $\boldsymbol{\psi}_k(\boldsymbol{\xi}(\tau))$ denotes a rearrangement of the multidimensional Hermite orthogonal polynomials with respect to the Gaussian function, which generates a complete basis in the random variable space. The orthogonality relationship is expressed as

$$E[\psi_i(\boldsymbol{\xi}), \psi_j(\boldsymbol{\xi})] = \int_{\Omega} \rho(\boldsymbol{\xi}) \psi_i(\boldsymbol{\xi}) \psi_j(\boldsymbol{\xi}) d\boldsymbol{\xi} = \delta_{ij} E[\Psi_k^2(\boldsymbol{\xi})] \tag{7}$$

with $E[\cdot]$ represents the expectancy operator in the probability space, $\rho(\boldsymbol{\xi})$ is the probability density function (PDF) or weight function, and δ_{ij} means the Kronecker delta product. For normal variables, $\boldsymbol{\psi}_k(\boldsymbol{\xi}(\tau))$ is the Hermite polynomials, denoted by

$$H(\boldsymbol{\xi}) = (-1)^m e^{\frac{\boldsymbol{\xi}^T \boldsymbol{\xi}}{2}} \left[\frac{\partial^p}{\partial \xi_{k_1}, \ \ldots, \partial \xi_{k_n}} e^{-\frac{\boldsymbol{\xi}^T \boldsymbol{\xi}}{2}} \right] \tag{8}$$

where m is the order and thus $\rho(\boldsymbol{\xi})$ is Gaussian associated. It should be noted that only finite order approximation is possible in practical implementation. If truncation order m is used in Eq. (6), the number of PC coefficients is

$$N = \frac{(m+n)!}{m!n!} - 1 \tag{9}$$

The mean-square sense error of the truncation can be given by

$$\lim_{m \to \infty} \left(E\left(\sum_{k=0}^{N} g_k \boldsymbol{\psi}_k(\boldsymbol{\xi}) - G(\boldsymbol{\xi}) \right)^2 \right) = 0 \tag{10}$$

The PC coefficients in Eq. (6) can be calculated by the Galerkin projection method [40], stochastic collocation method [37], and the quadrature technique [38]. The Galerkin method is intrusive, which requires modification to the established solver. The stochastic collocation and quadrature methods are non-intrusive, and the latter is recommended for advantages in post-processing [42]. Thus, we have

$$g_k = \frac{1}{E[\Psi_k^2(\boldsymbol{\xi})]} \int_{\Omega_1} \int_{\Omega_2} \cdots \int_{\Omega_n} G(\boldsymbol{\xi}) \Psi_k(\boldsymbol{\xi}) \rho_1(\xi_1) \cdots \rho_n(\xi_n) d\xi_1 \cdots d\xi_n \tag{11}$$

where $\Omega_1, \Omega_2, \ldots, \Omega_n$ are the sample spaces defined by the probability space of each stochastic variable. Variance $E[\Psi_k^2(\boldsymbol{\xi})]$ only needs to be evaluated once in different simulations, and it is independent of the stochastic journal bearing. The Gauss–Hermite quadrature is introduced to calculate the continuous integration numerically as

$$\int_{\Omega} \rho(\xi) G(\xi) \Psi_k(\xi) d\xi = \frac{1}{\sqrt{2\pi}} \sum_{i=0}^{r} \Xi_i G(\tilde{\xi}_i) \Psi_k(\tilde{\xi}_i) \tag{12}$$

where r is the number of quadrature points and should be larger than truncation order m, i.e., $r \geq m+1$, $\tilde{\xi}_i$ represents the quadrature points, which can be calculated as the zeros of Hermite polynomials with the required order, as denoted in Eq. (8), and $\Psi_k(\tilde{\xi}_i)$ is the value of polynomial chaos at $\tilde{\xi}_i$. The quadrature coefficient Ξ_i is fully determined by Hermite polynomials as

$$\Xi_i = \sqrt{\pi} \frac{2^{r+2}(r+1)!}{[H'_{r+1}(\tilde{\xi}_i)^2]} \tag{13}$$

It should be noted that Eq. (12) calculates one stochastic dimension of the integration. For the multiple stochastic parameters, the tensor product form quadrature is implemented on a one-dimensional basis. The computational burden is low for problems with a few stochasticity dimensions, no greater than 3, for instance. When the stochasticity has high dimensions, the sparse grid technique can be used to reduce the cost significantly [37,42]. The sample lubrication characteristics at the quadrature point $G(\tilde{\xi}_i)$ can be evaluated by the realizations of the deterministic Reynolds equation expressed in Eq. (3) by assigning the stochastic parameters to a specific point $\tilde{\xi}_i$. For convenience in the following formulation, the quadrature points form a vector and are quoted in general as $\tilde{\boldsymbol{\xi}}$.

At the quadrature point for all stochastic parameters $\tilde{\boldsymbol{\xi}}$, the theoretical misaligned journal bearing model is no longer subject to variability. In other words, a transformed set of deterministic PDEs should be solved. The finite difference method (FDM) coupled with the successive over-relaxation (SOR) method is

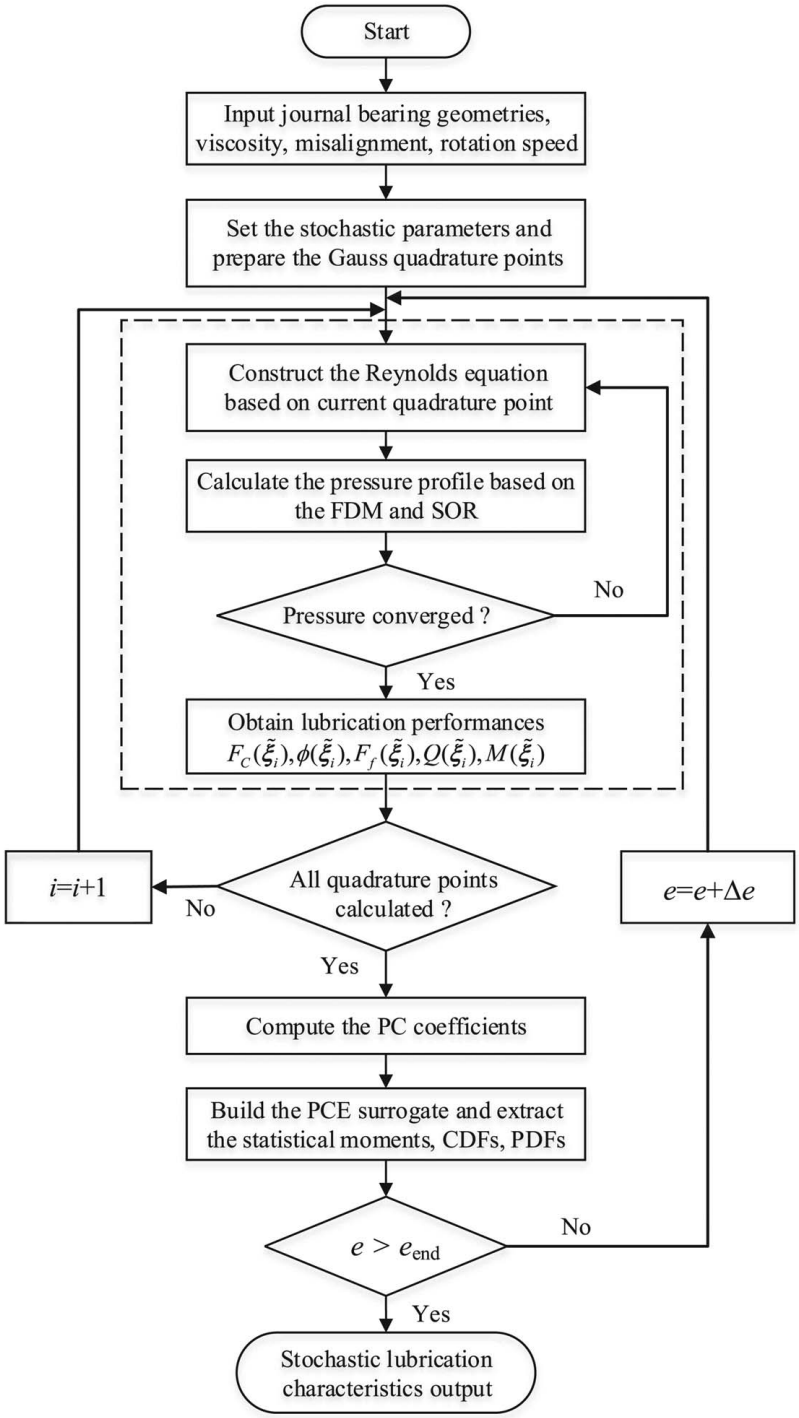

Fig. 2 Computation procedure of the stochastic lubrication characteristics

used to obtain the pressure profile. The boundary conditions used for iteration are [43]

$$p(0, z) = p(2\pi, z) = p(\varphi, -L/2) = p(\varphi, L/2) = 0 \tag{14}$$

The pressure will be assigned to atmosphere pressure if its value is negative in the iterations since the oil film cannot bear tensile loads. After calculation of the pressure distribution in the bearing clearance, the oil-film forces along and perpendicular to the journal centerline can be obtained as [34]

$$F_x(\tilde{\boldsymbol{\xi}}) = -\int_{-L/2}^{L/2}\int_0^{2\pi} p(\tilde{\boldsymbol{\xi}})R\sin\varphi d\varphi dz \tag{15}$$

$$F_y(\tilde{\boldsymbol{\xi}}) = -\int_{-L/2}^{L/2}\int_0^{2\pi} p(\tilde{\boldsymbol{\xi}})R\cos\varphi d\varphi dz \tag{16}$$

Then, the load-carrying capacity and attitude angle are given by

$$F_C(\tilde{\boldsymbol{\xi}}) = \sqrt{F_x^2(\tilde{\boldsymbol{\xi}}) + F_y^2(\tilde{\boldsymbol{\xi}})} \tag{17}$$

$$\phi(\tilde{\boldsymbol{\xi}}) = \tan^{-1}\left(\frac{F_x(\tilde{\boldsymbol{\xi}})}{F_y(\tilde{\boldsymbol{\xi}})}\right) \tag{18}$$

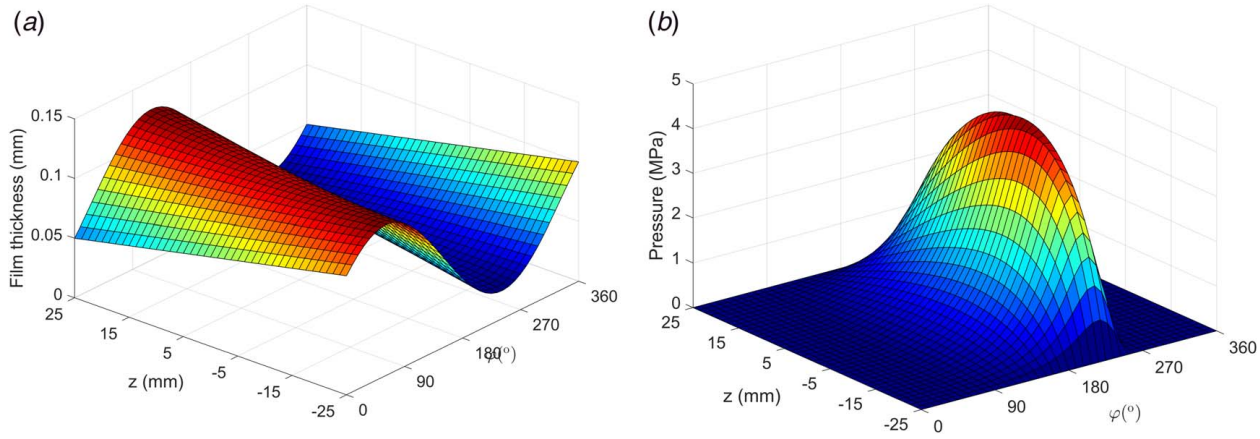

Fig. 3 Hydrodynamic performance of the journal bearing with misalignment: (*a*) oil-film thickness distribution and (*b*) pressure distribution

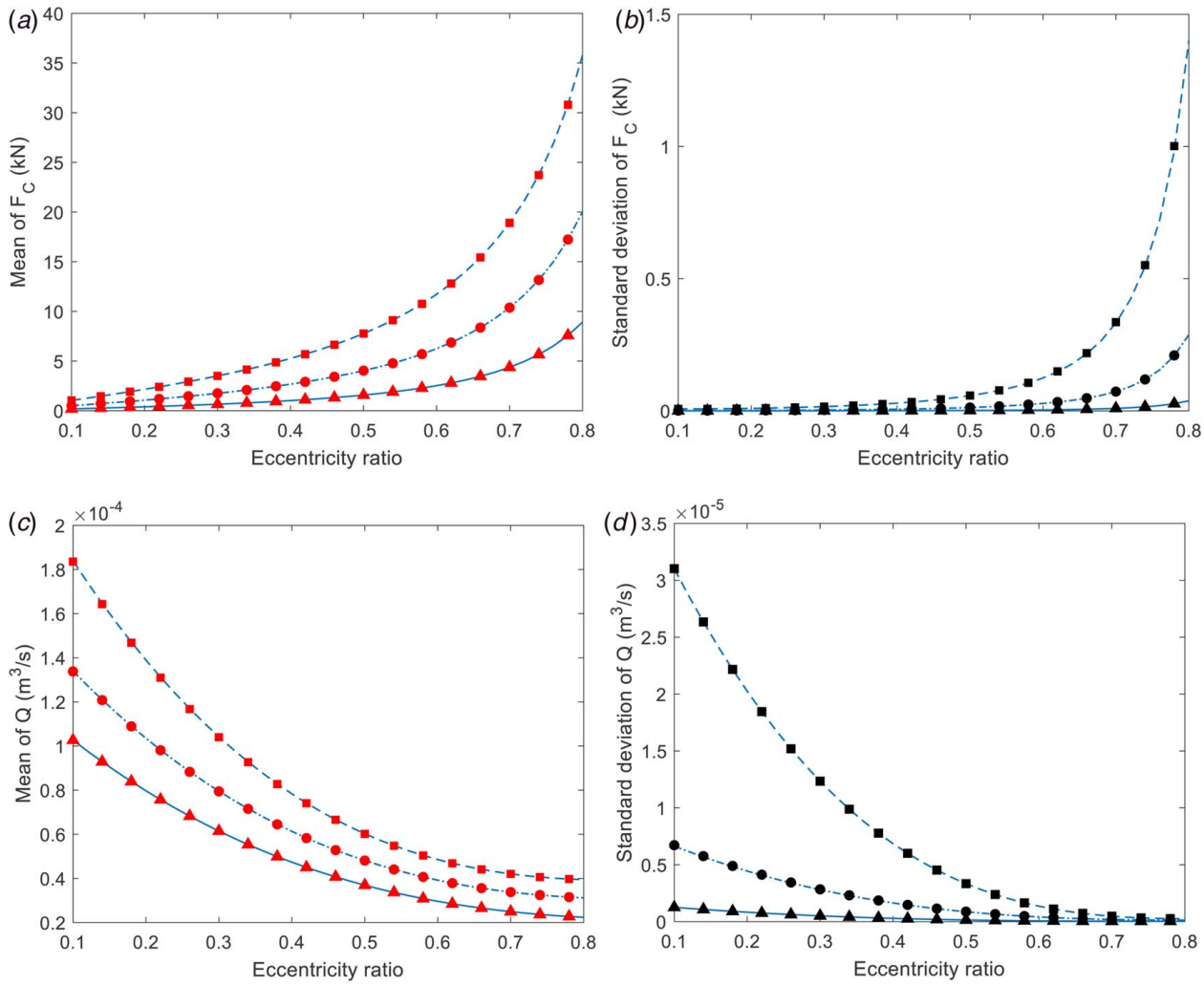

Fig. 4 Stochastic lubrication characteristics considering 10% variability in the misalignment magnitude (solid line-PCE with $L = 35$ mm; dash-dotted line-PCE with $L = 50$ mm; dashed line-PCE with $L = 65$ mm; -MCS with $L = 35$ mm; -MCS with $L = 50$ mm; -MCS with $L = 65$ mm): (*a*) mean of load-carrying capacity, (*b*) standard deviation of load-carrying capacity, (*c*) mean of end leakage flowrate, and (*d*) standard deviation of end leakage flowrate

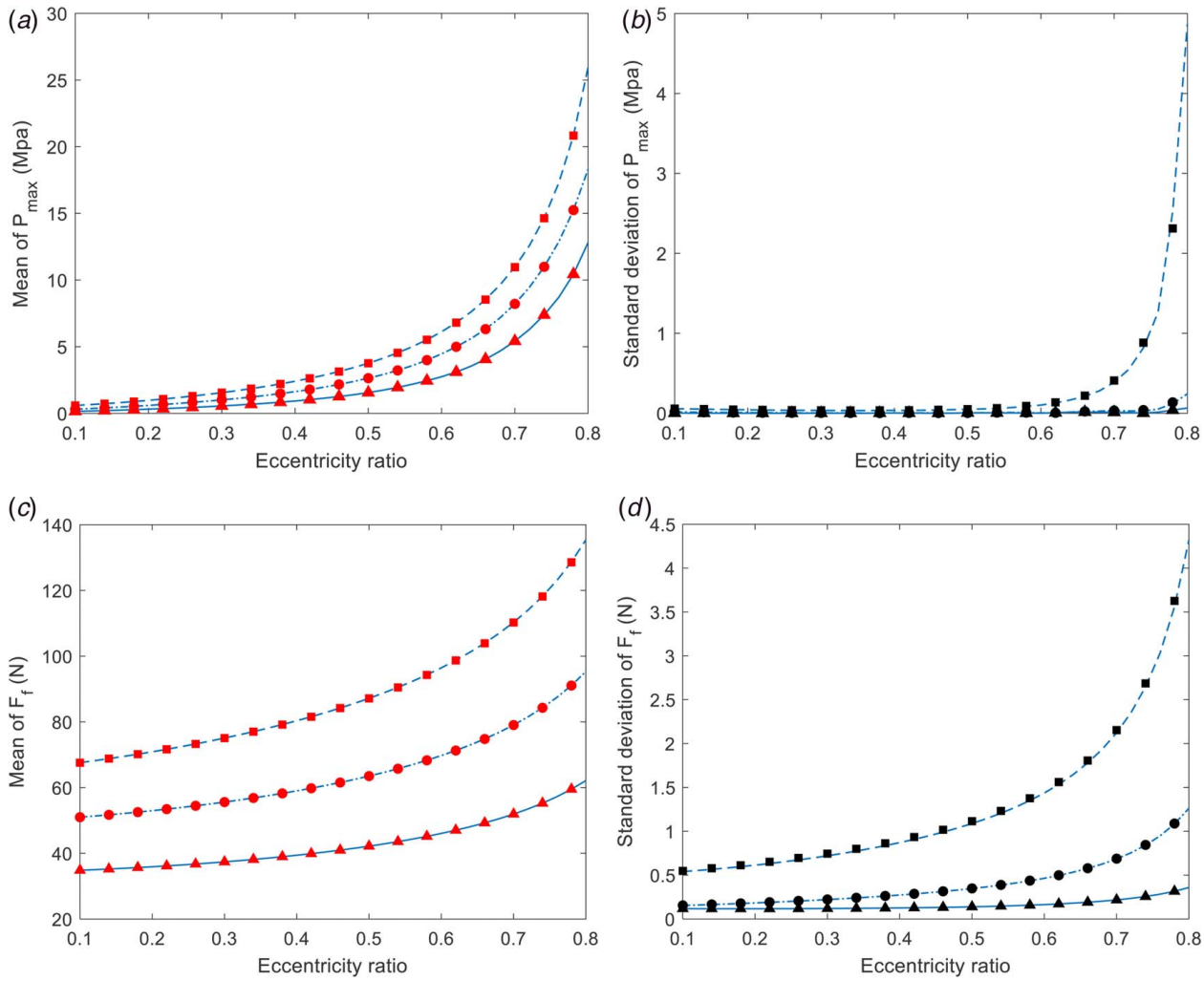

Fig. 5 Stochastic lubrication characteristics considering 10% variability in the misalignment magnitude (solid line-PCE with $L = 35$ mm; dash-dotted line-PCE with $L = 50$ mm; dashed line-PCE with $L = 65$ mm; -MCS with $L = 35$ mm; -MCS with $L = 50$ mm; -MCS with $L = 65$ mm): (*a*) mean of maximum pressure, (*b*) standard deviation of maximum pressure, (*c*) mean of friction force, and (*d*) standard deviation of friction force

On the moving surface, the friction force is expressed as

$$F_f(\tilde{\boldsymbol{\xi}}) = \int_{-L/2}^{L/2}\int_0^{2\pi}\left(\frac{h(\tilde{\boldsymbol{\xi}})}{2}\frac{\partial p(\tilde{\boldsymbol{\xi}})}{R\partial\varphi} + \frac{\mu(\tilde{\boldsymbol{\xi}})}{h(\tilde{\boldsymbol{\xi}})}R\omega\right)Rd\varphi dz \tag{19}$$

The lubricant flowrates are computed from the following formulas:

$$Q_1(\tilde{\boldsymbol{\xi}}) = -\int_0^{2\pi}\left(\frac{h^3(\tilde{\boldsymbol{\xi}})}{12\mu(\tilde{\boldsymbol{\xi}})}\frac{\partial p(\tilde{\boldsymbol{\xi}})}{\partial z}\bigg|_{z=-L/2}\right)Rd\varphi \tag{20}$$

$$Q_2(\tilde{\boldsymbol{\xi}}) = -\int_0^{2\pi}\left(\frac{h^3(\tilde{\boldsymbol{\xi}})}{12\mu(\tilde{\boldsymbol{\xi}})}\frac{\partial p(\tilde{\boldsymbol{\xi}})}{\partial z}\bigg|_{z=L/2}\right)Rd\varphi \tag{21}$$

$$Q(\tilde{\boldsymbol{\xi}}) = Q_1(\tilde{\boldsymbol{\xi}}) + Q_2(\tilde{\boldsymbol{\xi}}) \tag{22}$$

where $Q_1(\tilde{\boldsymbol{\xi}})$ and $Q_2(\tilde{\boldsymbol{\xi}})$ are the flowrates of the front-end and rear-end planes, and $Q(\tilde{\boldsymbol{\xi}})$ is the total leakage flowrate of the journal bearing.

The misalignment moments around the X and Z axes can be defined by

$$M_x(\tilde{\boldsymbol{\xi}}) = \int_{-L/2}^{L/2}\int_0^{2\pi} p(\tilde{\boldsymbol{\xi}})zR\cos\varphi d\varphi dz \tag{23}$$

$$M_y(\tilde{\boldsymbol{\xi}}) = \int_{-L/2}^{L/2}\int_0^{2\pi} p(\tilde{\boldsymbol{\xi}})zR\sin\varphi d\varphi dz \tag{24}$$

and the magnitude of moments is given as

$$M(\tilde{\boldsymbol{\xi}}) = \sqrt{M_x^2(\tilde{\boldsymbol{\xi}}) + M_y^2(\tilde{\boldsymbol{\xi}})} \tag{25}$$

Once all the sampled lubrication characteristics at quadrature points are obtained, the PC coefficients can be calculated and the PCE expression in Eq. (6) is fully determined which can also be termed the non-intrusive surrogate model. Based on the surrogate, the first two statistical moments of the stochastic lubrication characteristics, i.e., the ensemble mean and variance, can be given as

$$\text{Mean}(G(\boldsymbol{\xi})) = E[G(\boldsymbol{\xi})] = \int_\Omega \rho(\boldsymbol{\xi})G(\boldsymbol{\xi})d\boldsymbol{\xi} \tag{26}$$

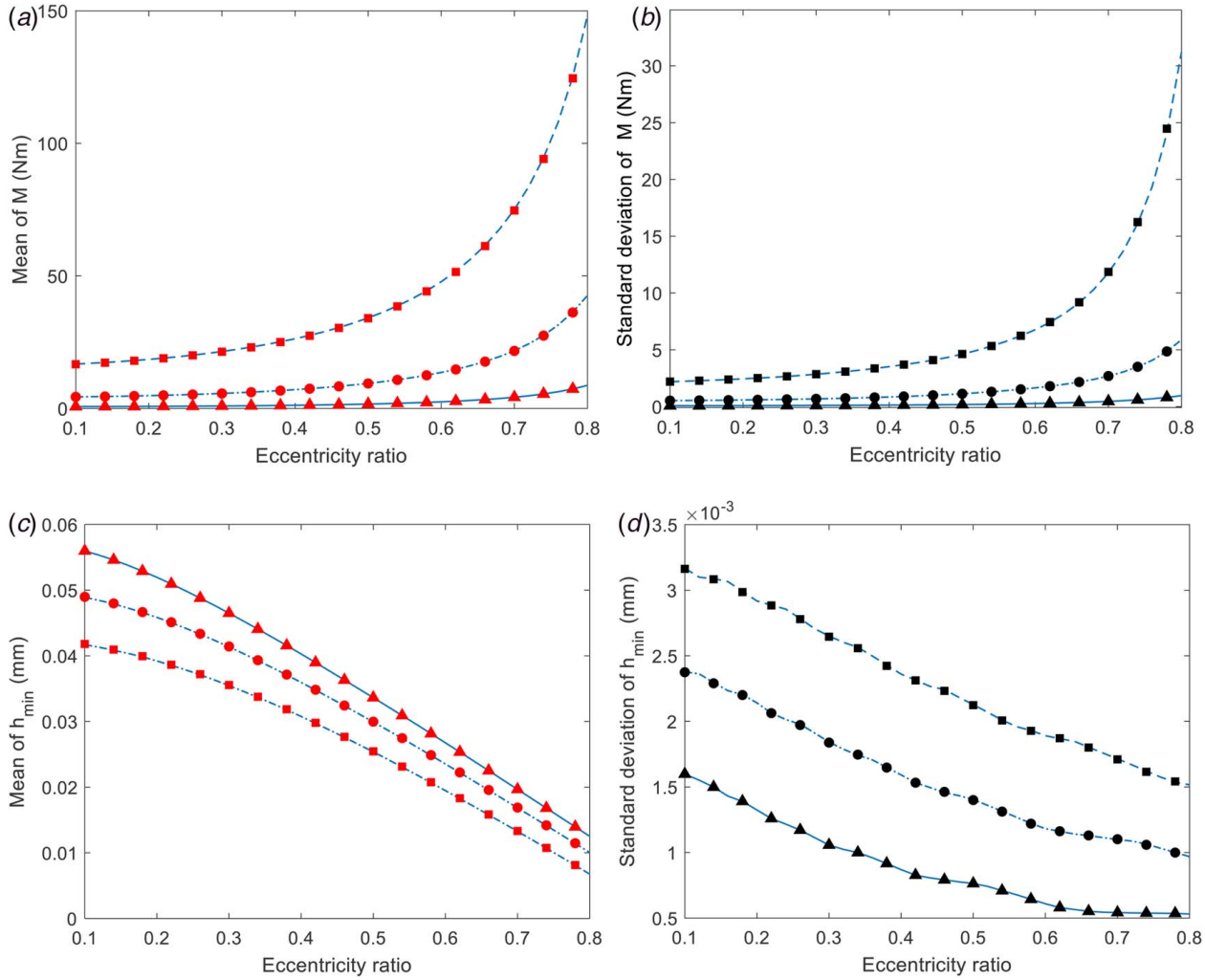

Fig. 6 Stochastic lubrication characteristics considering 10% variability in the misalignment magnitude (solid line-PCE with $L = 35$ mm; dash-dotted line-PCE with $L = 50$ mm; dashed line-PCE with $L = 65$ mm; -MCS with $L = 35$ mm; -MCS with $L = 50$ mm; and -MCS with $L = 65$ mm): (*a*) mean of misalignment moment, (*b*) standard deviation of misalignment moment, (c) mean of least film thickness, and (*d*) standard deviation of least film thickness

$$\mathrm{Var}(G(\boldsymbol{\xi})) = E[(G(\boldsymbol{\xi}) - E[G(\boldsymbol{\xi})])^2] = \int_{\Omega} \rho(\boldsymbol{\xi})(G(\boldsymbol{\xi}) - E[G(\boldsymbol{\xi})])^2 d\boldsymbol{\xi} \tag{27}$$

Further calculation yields

$$\mathrm{Mean}(G(\boldsymbol{\xi})) = g_0 \tag{28}$$

$$\mathrm{Var}(G(\boldsymbol{\xi})) = \sum_{i=1}^{N} g_i^2 E[\Psi_i^2(\boldsymbol{\xi}_i)] \tag{29}$$

Further, the PDFs and cumulative distribution functions (CDFs) of the lubrication characteristics can be calculated via the MCS based on the explicit surrogate without much computational cost. It can be noticed that the established solver of the PDE is called only at the quadrature points as a black box, which brings convenience in applications. For easier comprehension, the flowchart of the stochastic analysis scheme is provided in Fig. 2.

For engineering structures, the Gaussian model will provide a trustworthy approach to govern the variations of uncertainties. It should be noted that the physical parameters of the bearing system are strictly positive and in a reasonable range. In actual implementation, the random samples of uncertain journal bearing parameters that have negative values should be removed. This is to ensure the analysis is physically correct, although the results will generally not be affected (i.e., the probability of the uncertainty taking an unreasonable value is very low, such as negative numbers).

For comparison and validation of the stochastic lubrication characteristics obtained by the PCE frame, the crude MCS is also applied to the misaligned journal bearing model. Suppose κ random samples are drawn for the simulation, the obtained statistical moments are given as

$$\begin{cases} \bar{G}_{MCS} = \dfrac{1}{\kappa}\displaystyle\sum_{i=1}^{\kappa} G(\underline{\boldsymbol{\xi}}_i) \\ \boldsymbol{\sigma}^2_{MCS} = \dfrac{1}{\kappa - 1}\displaystyle\sum_{i=1}^{\kappa} (G(\underline{\boldsymbol{\xi}}_i) - \bar{G}_{MCS})^2 \end{cases} \tag{30}$$

where $\underline{\boldsymbol{\xi}}_i$, $i = 1, 2, \ldots, \kappa$ means the parameter samples for the MCS. Moreover, the PDFs and CDFs can be inferred from the output characteristics samples $G(\underline{\boldsymbol{\xi}})$.

4 Results and Discussion

In this section, the numerical investigations and relevant discussion about stochastic lubrication under different parameter

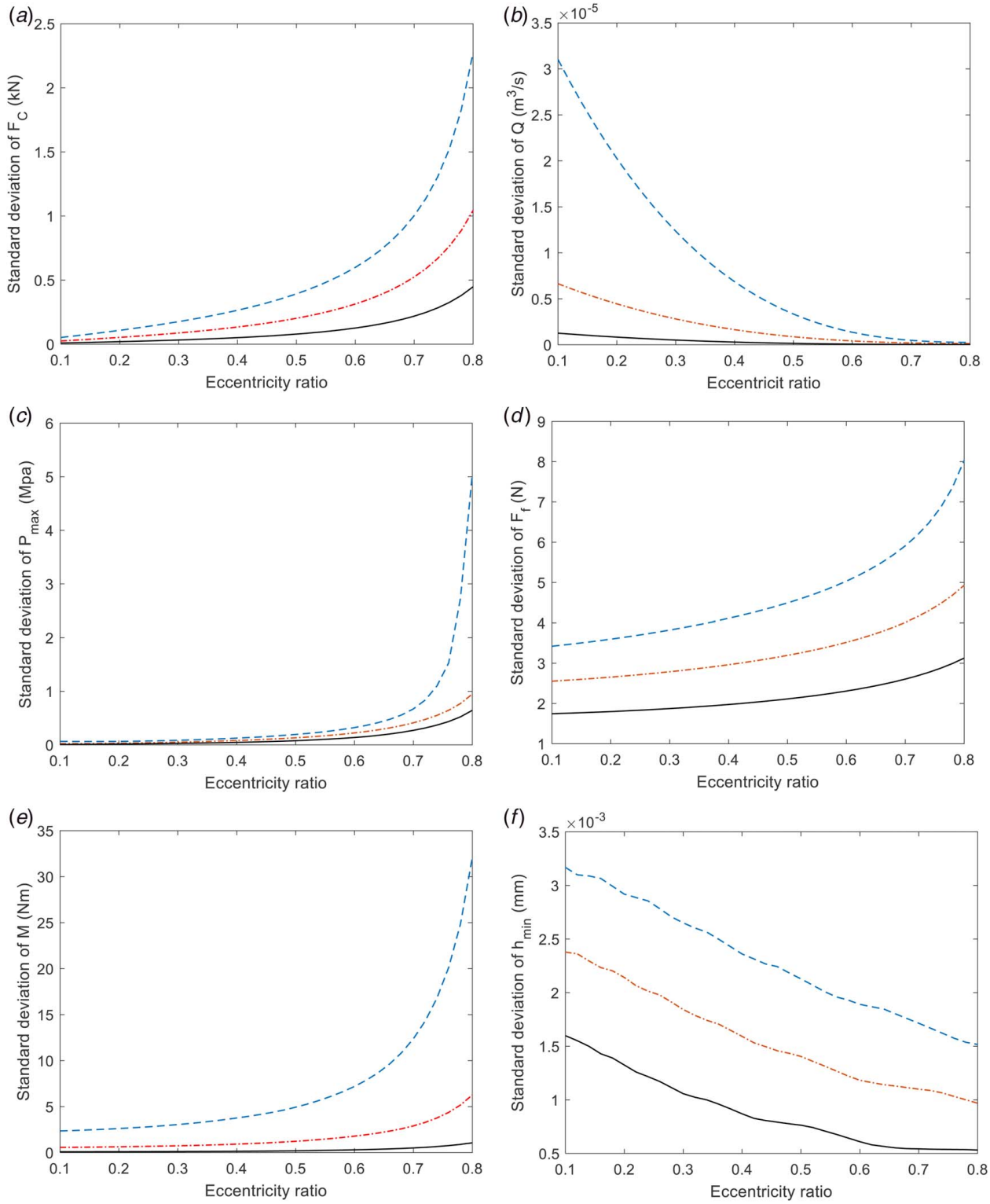

Fig. 7 Standard deviations of lubrication characteristics considering variabilities in the misalignment magnitude and lubricant viscosity (solid line-*L* = 35 mm; dash-dotted line-*L* = 50 mm; dashed line-*L* = 65 mm): (*a*) load-carrying capacity, (*b*) end leakage flowrate, (c) maximum pressure, (*d*) friction force, (*e*) misalignment moment, and (*f*) least film thickness

variabilities are presented. During the simulation, the deterministic journal bearing model parameters are as follows: bearing clearance $c = 0.075$ mm, bearing diameter $D = 70$ mm, viscosity of lubricant $\mu = 0.03$ Pa · s, angular rotating speed $\omega = 3000$ r/min, misalignment magnitude $\gamma = 0.001$ rad, and misalignment angle $\alpha = \varphi_0 = 90$ deg. The bearing width is varied for different cases to show the lubrication characteristics with different length-to-width ratios and will be given later.

First, a deterministic illustration of the misaligned journal bearing without uncertainty is provided to indicate the effects of misalignment. In Figs. 3(*a*) and 3(*b*), the thickness of oil film in the clearance and its corresponding pressure distribution are plotted with a bearing width $L = 50$ mm when the eccentricity ratio in the midplane is $e_0 = 0.6$. It is shown that the journal misalignment has critical influences on the lubrication performance of the system. The distribution of the oil film, as well as pressure, is inclined compared

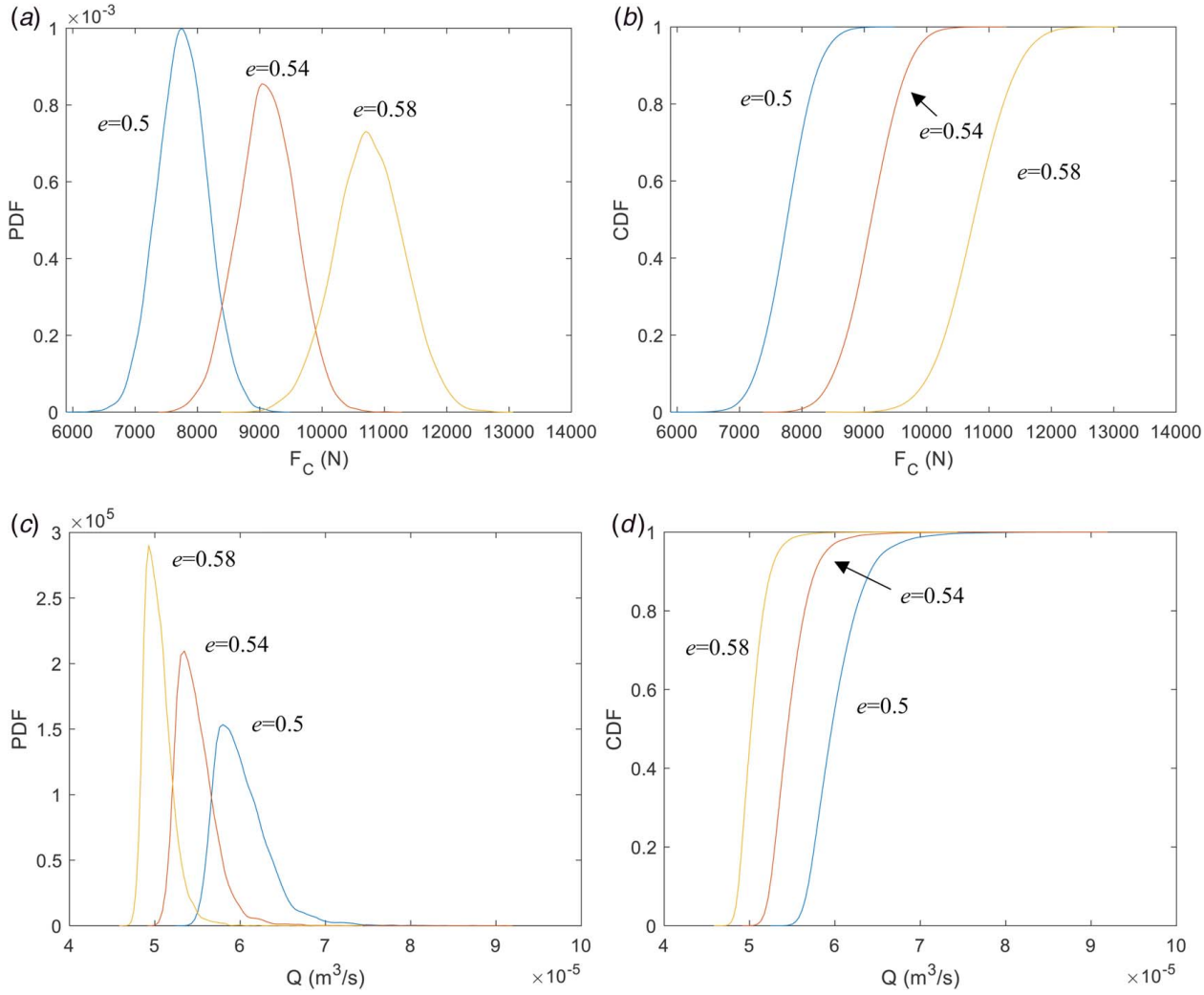

Fig. 8 Stochastic lubrication characteristics considering variabilities in the misalignment magnitude and lubricant viscosity with $L = 50$ mm: (*a*) PDF of load-carrying capacity, (*b*) CDF of load-carrying capacity, (*c*) PDF of end leakage flowrate, and (*d*) CDF of end leakage flowrate

with aligned journal bearings and they are closely related to the magnitude of misalignment. The location of the highest pressure is shifted, and two peaks may occur in certain cases [12]. It can cause possible direct contact of the shaft and bearing if the misalignment is significant and thus affects the corresponding rotordynamics. In the following, comprehensive stochastic analyses of the journal bearing will be carried out considering individual or multi-parameter deviations.

To include the influence of the bearing geometries, three different bearing widths are considered for stochastic investigations, i.e., $L =$ 35, 50 and 65 mm. The misalignment in a journal bearing can be caused by many factors and it evolves with service time. In other words, it can be difficult to measure precisely, or it changes inherently. Naturally, it requires a robust treatment of stochasticity. The value of dispersion is adopted as 10% in this paper, and the reasons are twofold. First, it is a relatively large degree and can show the excellent performance of the PCE method (techniques such as perturbation method can only handle small variations). Second, this value represents one of the typical fluctuation levels which have been used in uncertainty propagations. Based on the established scheme previously, the lubrication performance parameters (i.e., their ensemble mean and standard deviation) under a 10% dispersion of the misalignment magnitude are plotted in Figs. 4–6, including the load-carrying capacity, end leakage rate, maximum pressure, friction force, misalignment moment, and the least film thickness. In the figures, solid lines denote the results for $L = 35$ mm, dash-dotted lines for $L = 50$ mm, and dashed lines for $L = 65$ mm using the PCE while triangle, circle, and square markers are the corresponding results from the MCS with 1000 samples. For comparison purposes, the solutions from the MCS need to be accurate enough. Here, the MCS results are verified to be convergent using 1500 samples, which are not presented to avoid duplication of figures. It is worth pointing out that only partial points from the MCS are presented in the figures for the sake of clarity. The crude MCS will serve as a reference for the accuracy validation, and its efficacy is believed to be much lower than that of the PCE due to its low convergence rate. Specifically, only an order 5 is used in the PCE requiring six realizations of the deterministic Reynolds equations while 1000 realizations in the MCS are needed. Consequently, the running time could be reduced more than 100 times. From Figs. 4–6, we can notice that the established stochastic frame has the same accuracy as the crude MCS since the results obtained from the two agree with each other perfectly for both the mean and standard deviation. The above two aspects confirm the numerical performance of the PCE analysis scheme, and we can now focus on the stochastic characteristics of the results. As shown in Figs. 4(*a*) and 4(*b*) with different line types, longer bearing width can provide greater load-carrying capacity, and also, the deviation is more significant under the same stochasticity input. Generally, the deviation ability of load capacity of the journal bearing with

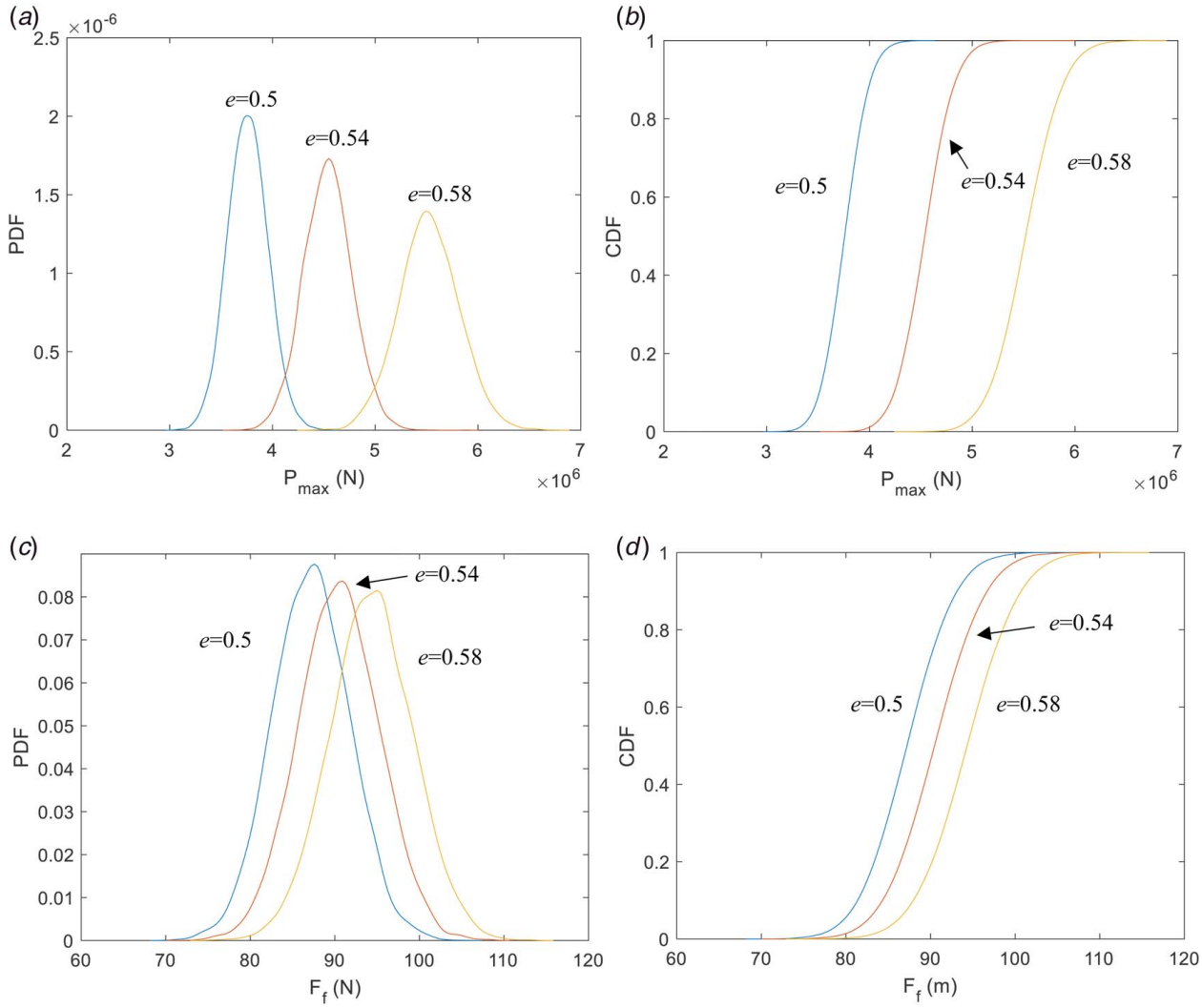

Fig. 9 Stochastic lubrication characteristics considering variabilities in the misalignment magnitude and lubricant viscosity with $L = 50$ mm: (*a*) PDF of maximum pressure, (*b*) CDF of maximum pressure, (*c*) PDF of friction force, and (*d*) CDF of friction force

$L = 35$ mm shows little influence of the uncertain parameter while it is notable for $L = 65$ mm. This feature applies to all of the lubrication parameters. Moreover, the magnitudes of load-carrying capacity and its standard deviation increase with the eccentricity ratio. Contrary trends have been found in Figs. 4(*c*) and 4(*d*) for the mean and standard variance of the end leakage rate, where the mean increases with the increase of eccentricity ratio and the standard variance decrease with it. This phenomenon is caused by journal misalignment effects in high eccentricity ratio as evidenced in literature [12]. The longer the bearing width, the higher the end leakage rate. In the low eccentricity ratio range, the standard deviation of Q is large while it is trivial in high ratio ranges. The maximum pressure shows a similar phenomenon with the load-carrying capacity though the bearing width has caused less deviation of maximum pressure in the deterministic sense, as indicated in Fig. 5(*a*). However, it is observed in Fig. 5(*b*) that for the bearing width 35 and 50 mm the standard deviations are very small while for larger width 65 mm it rallies up for high eccentricity ratios. In Figs. 5(*c*) and 5(*d*) and 6(*a*) and 6(*b*), the mean and standard variance of the friction force and misalignment moment are given. They share a similar stochastic pattern as evidenced in load-carrying capacity except that the mean friction force is evenly distributed concerning different bearing widths. From Figs. 6(*c*) and 6(*d*), distinctive features are found for the stochastic least oil-film thickness; i.e., its standard deviations are linearly decreasing when the eccentricity ratio increases while all others exhibit nonlinear relationships.

Next, we consider simultaneous effects of stochastic misalignment magnitude and lubricant viscosity, which represents a combined case. The latter has been commonly treated uncertain in literature to consider variable working conditions, in which the temperature is to some extent unpredictable and causes fluctuations in viscosity. It should be noted that the mean value or the first-order statistical moment of stochastic lubrication performance should be equal to the deterministic one, which is essential from a probability point of view. In other words, they are the same no matter what stochastic parameters are considered. Thus, the mean of all the lubrication parameters will not be shown to save space. Suppose both of the two stochastic uncertainties have the same 10% variabilities of their respective nominal values, the standard deviations of the aforementioned lubrication performance parameters are demonstrated in Fig. 7 for the three bearing widths. In Fig. 7, the dashed lines show the standard variance with $L = 65$ mm, dash dotted lines represent results for $L = 50$ mm, and solid lines for $L = 35$ mm. It can be noted that all the stochastic lubrication characteristics show more severe deviations compared with the single uncertainty case, which suggests the fact that multiple uncertainties may cause the journal bearing to produce the practical performance that

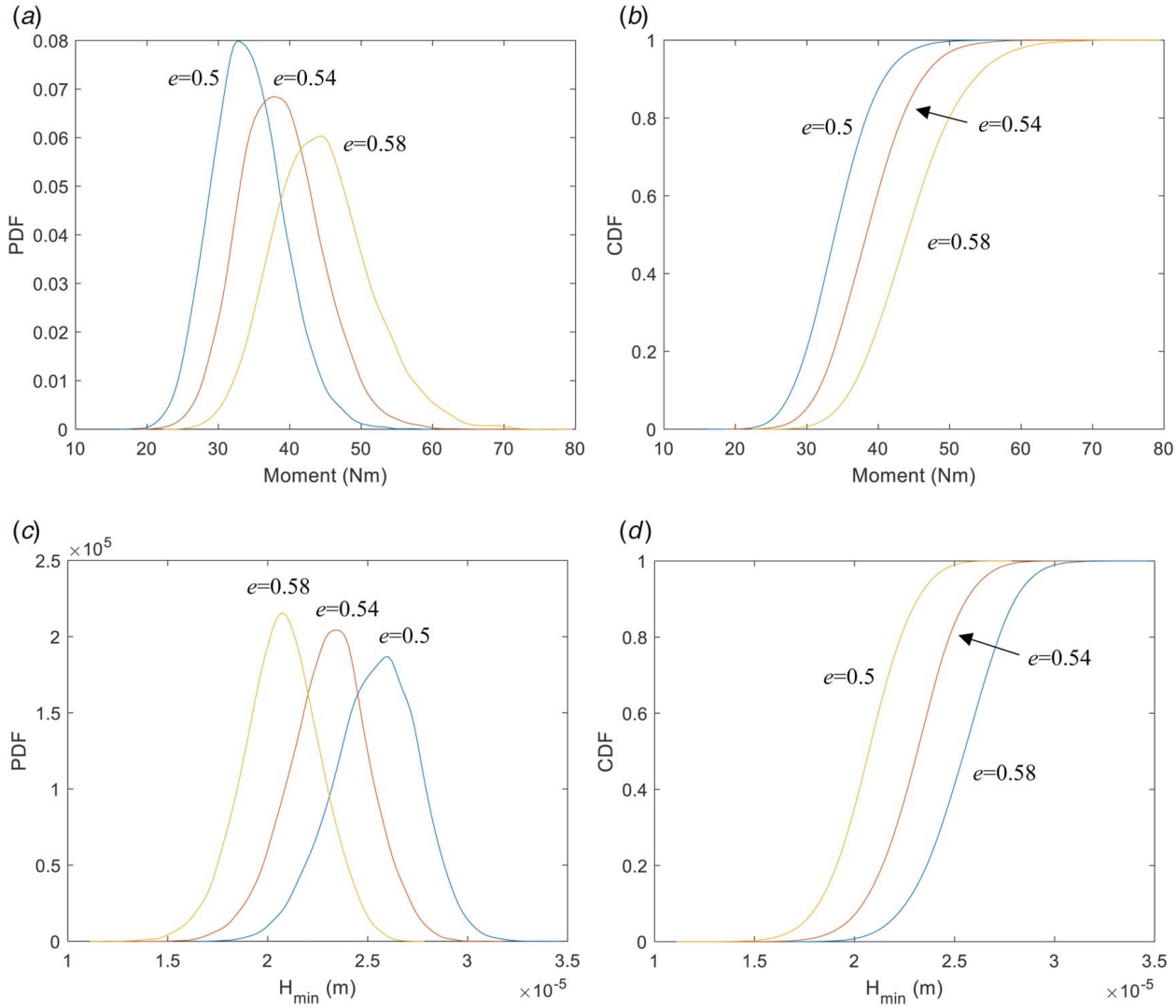

Fig. 10 Stochastic lubrication characteristics considering variabilities in the misalignment magnitude and lubricant viscosity with $L = 50$ mm: (*a*) PDF of misalignment moment, (*b*) CDF of misalignment moment, (c) PDF of least film thickness, and (*d*) CDF of least film thickness

is significantly unexpected. The previously found feature is also valid in multi-uncertainties cases: the wider bearing width, the greater variability of the journal bearing lubrication parameters. That is caused by the lubricating nature. It should be noted that the mean values of stochastic lubrication performance should be equal to the deterministic ones, which is essential from a probabilistic point of view. In other words, they are the same no matter what stochastic parameters are considered. Thus, the mean curves of all the lubrication parameters are not shown to avoid duplication.

An important merit of the stochastic analysis over the non-probabilistic methods is that a complete set of distribution information can be obtained, i.e., the arbitrary orders of statistical moments. Moreover, we can infer the PDFs and CDFs of the stochastic outputs, which provide informatic knowledge of the stochastic system. Specifically, the PDF indicates the probability of a variable to take certain values and it shows the sparsity. The CDF, taking the value from 0 to 1 inclusive, gives the cumulative probability of a variable for a distribution range no greater than certain values. With the two-dimensional uncertain inputs demonstrated in Fig. 7, the corresponding PDFs and CDFs are presented in Figs. 8–10 for with bearing width $L = 50$ mm when the eccentricity ratio is 0.5, 0.54 and 0.58. Figures 8(*a*) and 8(*b*) plot the results for the load-carrying capacity, in which the PDFs indicate that a larger eccentricity ratio will cause the magnitude of capacity to increase and the peak of probability to decrease. The decreasing of peak probability in turn leads to the wider distribution of the magnitude of capacity, which can be called sparsity. In other words, the load-carrying capacity has higher probabilities in a wider range. Essentially, the CDFs reflect these features conferring to the PDF plots. The distributions of the end leakage rate are more concentrated, as shown in Figs. 8(*c*) and 8(*d*), showing fewer deviation degrees or sparsity caused by the uncertainties. Consequently, the CDFs increase rapidly to 1. The variation pattern for the maximum pressure in Figs. 9(*a*) and 9(*b*) is similar to that of the load-carrying capacity. The magnitude of maximum pressure increases with the eccentricity ratio dramatically. As evidenced in Figs. 9(*c*) and 9(*d*), the friction force is widely distributed as a result of multiple uncertainties while the probability distribution is barely affected by the eccentricity ratio. For misalignment moments shown in Figs. 10(*a*) and 10(*b*), however, the eccentricity ratio will cause the probability distribution to expand significantly and peak values to decrease. That is, the more the shaft center is shifted, the wider the distribution range of misalignment moment along with an increase of magnitudes in overall ranges. The propagation mechanism for the uncertain least film thickness demonstrated in Figs. 10(*c*) and 10(*d*) is characterized the same way as the friction force despite that the effects of the eccentricity ratio are in an inversed manner. Moreover, the fluid–asperity interaction

is an important behavior in the hydrodynamic lubrication regime and often causes high-frequency resonances [44,45]. In the future, further efforts will be devoted to clarifying the intrinsic interaction between the stochasticity of physical parameters and fluid–asperity interaction.

5 Conclusion

This paper investigates the stochastic lubrication characteristics of a cylindrical hydrodynamic journal bearing with angular misalignment considering uncertainties in critical model parameters. The PCE is employed for efficient uncertainty propagation analysis, which is validated by the crude MCS. It should be noted that the non-intrusive PCE is much faster than the crude MCS. Comprehensive performances are studied including the load-carrying capacity, end leakage rate, maximum pressure, friction force, misalignment moment, and least film thickness. In-depth discussions are performed to reveal the stochastic properties of the misaligned journal bearing using the first two orders statistical moments. The PDFs and CDFs of the performance parameters for three specific journal eccentricities are extracted from the PCE results. The standard variations of lubrication performance parameters of long bearings are higher than short bearings. Moreover, the standard variations of the load-carrying capacity, maximum pressure, friction force and misalignment moment increase rapidly with the increase of eccentricity while those of the end leakage flowrate and least film thickness decrease with it.

The application of the non-intrusive PCE to the stochastic lubrication analysis of a misaligned journal bearing enables the efficient computation of journal bearings within various contexts, such as journal bearing with surface roughness or rotor-bearing systems. The findings indicate that the stochasticity in journal bearing parameters will cause serious deviations of the hydrodynamic lubrication performances.

Acknowledgment

This research was supported by the Fundamental Research Funds for the Central Universities (Grant No. G2021KY0601) and the National Natural Science Foundation of China (Grant Nos. 11972295 and 12072263).

Conflict of Interest

There are no conflicts of interest.

Data Availability Statement

The authors attest that all data for this study are included in the paper.

References

[1] Ahmed, A., and El-Shafei, A., 2008, "Effect of Misalignment on the Characteristics of Journal Bearings," ASME J. Eng. Gas Turbines Power, **130**(4), p. 042501.

[2] Ma, J., Zhang, H., Lou, S., Chu, F., Shi, Z., Gu, F., and Ball, A. D., 2021, "Analytical and Experimental Investigation of Vibration Characteristics Induced by Tribofilm-Asperity Interactions in Hydrodynamic Journal Bearings," Mech. Syst. Signal Process, **150**, p. 107227.

[3] Kim, S., Shin, D., and Palazzolo, A. B., 2021, "A Review of Journal Bearing Induced Nonlinear Rotordynamic Vibrations," ASME J. Tribol., **143**(11), p. 111802.

[4] Zhang, Y., Li, X., Dang, C., Hei, D., Wang, X., and Lü, Y., 2019, "A Semianalytical Approach to Nonlinear Fluid Film Forces of a Hydrodynamic Journal Bearing With Two Axial Grooves," Appl. Math. Model., **65**, pp. 318–332.

[5] Zhou, W., Wei, X., Wang, L., and Wu, G., 2017, "A Superlinear Iteration Method for Calculation of Finite Length Journal Bearing's Static Equilibrium Position," R. Soc. Open Sci., **4**(5), p. 161059.

[6] Zhu, S., Sun, J., Li, B., Zhao, X., Wang, H., Teng, Q., Ren, Y., and Zhu, G., 2020, "Research on Turbulent Lubrication of Misaligned Journal Bearing Considering the Axial Motion of Journal," ASME J. Tribol., **142**(2), p. 021802.

[7] Sun, X., Sepahvand, K. K., and Marburg, S., 2021, "Stability Analysis of Rotor-Bearing Systems Under the Influence of Misalignment and Parameter Uncertainty," Appl. Sci., **11**(17), p. 7918.

[8] Jang, J. Y., and Khonsari, M. M., 2015, "On the Characteristics of Misaligned Journal Bearings," Lubricants, **3**(1), pp. 27–53.

[9] Pierre, I., de France, E., Bouyer, J., and Fillon, M., 2004, "Thermohydrodynamic Behavior of Misaligned Plain Journal Bearings: Theoretical and Experimental Approaches," Tribol. Trans., **47**(4), pp. 594–604.

[10] Ebrat, O., Mourelatos, Z. P., Vlahopoulos, N., and Vaidyanathan, K., 2004, "Calculation of Journal Bearing Dynamic Characteristics Including Journal Misalignment and Bearing Structural Deformation," Tribol. Trans., **47**(1), pp. 94–102.

[11] Xie, Z., Shen, N., Zhu, W., Tian, W., and Hao, L., 2021, "Theoretical and Experimental Investigation on the Influences of Misalignment on the Lubrication Performances and Lubrication Regimes Transition of Water Lubricated Bearing," Mech. Syst. Signal Process, **149**, p. 107211.

[12] Sun, J., and Gui, C., 2004, "Hydrodynamic Lubrication Analysis of Journal Bearing Considering Misalignment Caused by Shaft Deformation," Tribol. Int., **37**(10), pp. 841–848.

[13] Bouyer, J., and Fillon, M., 2002, "An Experimental Analysis of Misalignment Effects on Hydrodynamic Plain Journal Bearing Performances," ASME J. Tribol., **124**(2), pp. 313–319.

[14] He, Z., Zhang, J., Xie, W., Li, Z., and Zhang, G., 2012, "Misalignment Analysis of Journal Bearing Influenced by Asymmetric Deflection, Based on a Simple Stepped Shaft Model," J. Zhejiang Univ., Sci., A, **13**(9), pp. 647–664.

[15] Lv, F., Jiao, C., Ta, N., and Rao, Z., 2018, "Mixed-Lubrication Analysis of Misaligned Bearing Considering Turbulence," Tribol. Int., **119**, pp. 19–26.

[16] Das, S., and Guha, S. K., 2019, "Numerical Analysis of Steady-State Performance of Misaligned Journal Bearings With Turbulent Effect," J. Braz. Soc. Mech. Sci. Eng., **41**(2), p. 81.

[17] Zhu, S., Sun, J., Li, B., and Zhu, G., 2020, "Thermal Turbulent Lubrication Analysis of Rough Surface Journal Bearing With Journal Misalignment," Tribol. Int., **144**, p. 106109.

[18] Nikolakopoulos, P. G., and Papadopoulos, C. A., 2008, "A Study of Friction in Worn Misaligned Journal Bearings Under Severe Hydrodynamic Lubrication," Tribol. Int., **41**(6), pp. 461–472.

[19] Alves, D. S., Daniel, G. B., Castro, H. F. D., Machado, T. H., Cavalca, K. L., Gecgel, O., Dias, J. P., and Ekwaro-Osire, S., 2020, "Uncertainty Quantification in Deep Convolutional Neural Network Diagnostics of Journal Bearings With Ovalization Fault," Mech. Mach. Theory, **149**, p. 103835.

[20] Fu, C., Xu, Y., Yang, Y., Lu, K., Gu, F., and Ball, A., 2020, "Dynamics Analysis of a Hollow-Shaft Rotor System With an Open Crack Under Model Uncertainties," Commun. Nonlinear Sci. Numer. Simul., **83**, p. 105102.

[21] da Silva, H. A. P., and Nicoletti, R., 2019, "Design of Tilting-Pad Journal Bearings Considering Bearing Clearance Uncertainty and Reliability Analysis," ASME J. Tribol., **141**(1), p. 011703.

[22] Ruiz, R. O., and Diaz, S. E., 2016, "Effect of Uncertainties in the Estimation of Dynamic Coefficients on Tilting Pad Journal Bearings," Proceedings of the ASME 2016 International Mechanical Engineering Congress and Exposition, Phoenix, AZ, Nov. 11–17, American Society of Mechanical Engineers Digital Collection, p. V04BT05A030.

[23] Fu, C., Zhu, W., Yang, Y., Zhao, S., and Lu, K., 2022, "Surrogate Modeling for Dynamic Analysis of an Uncertain Notched Rotor System and Roles of Chebyshev Parameters," J. Sound Vib., **524**, **116755**.

[24] Wale, G., and Mba, D., 2005, "Identifying and Minimising Uncertainty for Experimental Journal Bearing Studies," Int. J. Rotating Mach., **2005**(3), pp. 221–231.

[25] Li, Z., Jiang, J., and Tian, Z., 2017, "Stochastic Dynamics of a Nonlinear Misaligned Rotor System Subject to Random Fluid-Induced Forces," ASME J. Comput. Nonlinear Dyn., **12**(1), p. 011004.

[26] Christensen, H., 1969, "Stochastic Models for Hydrodynamic Lubrication of Rough Surfaces," Proc. Inst. Mech. Eng., **184**(1), pp. 1013–1026.

[27] Mo, F., Shen, C., Zhou, J., and Khonsari, M. M., 2017, "Statistical Analysis of the Influence of Imperfect Texture Shape and Dimensional Uncertainty on Surface Texture Performance," IEEE Access, **5**, pp. 27023–27035.

[28] Dobrica, M. B., Fillon, M., and Maspeyrot, P., 2006, "Mixed Elastohydrodynamic Lubrication in a Partial Journal Bearing—Comparison Between Deterministic and Stochastic Models," ASME J. Tribol., **128**(4), pp. 778–788.

[29] Wierzcholski, K., and Miszczak, A., 2004, "Stochastic Model for Turbulent Lubrication of Slide Journal Bearing in Ship Technology," Mar. Technol. Trans., **15**, pp. 455–466.

[30] Cavalini, A. A., Jr., Lara-Molina, F. A., Sales, T. D. P., Koroishi, E. H., and Steffen, V., Jr., 2015, "Uncertainty Analysis of a Flexible Rotor Supported by Fluid Film Bearings," Lat Am. J. Solids Struct., **12**(8), pp. 1487–1504.

[31] Visnadi, L. B., and de Castro, H. F., 2019, "Influence of Bearing Clearance and Oil Temperature Uncertainties on the Stability Threshold of Cylindrical Journal Bearings," Mech. Mach. Theory, **134**, pp. 57–73.

[32] Tyminski, N. C., Tuckmantel, F. W., Cavalca, K. L., and de Castro, H. F., 2017, "Bayesian Inference Applied to Journal Bearing Parameter Identification," J. Braz. Soc. Mech. Sci. Eng., **39**(8), pp. 2983–3004.

[33] Koutsovasilis, P., and Schweizer, B., 2014, "Parameter Variation and Data Mining of Oil-Film Bearings: A Stochastic Study on the Reynolds's Equation of Lubrication," Arch. Appl. Mech., **84**(5), pp. 671–692.

[34] Maharshi, K., Mukhopadhyay, T., Roy, B., Roy, L., and Dey, S., 2018, "Stochastic Dynamic Behaviour of Hydrodynamic Journal Bearings Including the Effect of Surface Roughness," Int. J. Mech. Sci., **142**, pp. 370–383.
[35] Fu, C., Zhu, W., Zheng, Z., Sun, C., Yang, Y., and Lu, K., 2022, "Nonlinear Responses of a Dual-Rotor System With Rub-Impact Fault Subject to Interval Uncertain Parameters," Mech. Syst. Signal Process, **170**, p. 108827.
[36] Jacquelin, E., Friswell, M. I., Adhikari, S., Dessombz, O., and Sinou, J.-J., 2016, "Polynomial Chaos Expansion With Random and Fuzzy Variables," Mech. Syst. Signal Process, **75**, pp. 41–56.
[37] Garoli, G. Y., and Castro, H., 2016, "Stochastic Collocation Approach for Evaluation of Journal Bearing Dynamic Coefficients," Proceedings of the Proceedings of the 3rd International Symposium on Uncertainty Quantification and Stochastic Modeling, Maresias, Sao Paulo, Brazil, Feb. 15–19, pp. 1–10.
[38] Fu, C., Xu, Y., Yang, Y., Lu, K., Gu, F., and Ball, A., 2020, "Response Analysis of an Accelerating Unbalanced Rotating System With Both Random and Interval Variables," J. Sound Vib., **466**, p. 115047.
[39] Wang, X., Zhou, L., Huang, M., Yue, X., and Xu, Q., 2018, "Numerical Investigation of Journal Misalignment on the Static and Dynamic Characteristics of Aerostatic Journal Bearings," Measurement, **128**, pp. 314–324.
[40] Ghanem, R. G., and Spanos, P. D., 2003, *Stochastic Finite Elements: A Spectral Approach*, Courier Corporation, New York.
[41] Xiu, D., and Karniadakis, G. E., 2002, "The Wiener–Askey Polynomial Chaos for Stochastic Differential Equations," SIAM J. Sci. Comput., **24**(2), pp. 619–644.
[42] Blatman, G., and Sudret, B., 2011, "Adaptive Sparse Polynomial Chaos Expansion Based on Least Angle Regression," J. Comput. Phys., **230**(6), pp. 2345–2367.
[43] Li, J., Zhang, G., Huang, Y., Chen, R., Yan, S., and Cao, H., 2017, "Influence of Non-Gaussian-Distributed Surface Roughness on the Static Performance of Slider Bearings," Tribol. Trans., **60**(4), pp. 739–752.
[44] Ma, J., Zhang, H., Shi, Z., Chu, F., Gu, F., and Ball, A. D., 2021, "Modelling Acoustic Emissions Induced by Dynamic Fluid-Asperity Shearing in Hydrodynamic Lubrication Regime," Tribol. Int., **153**, p. 106590.
[45] Scaraggi, M., Angerhausen, J., Dorogin, L., Murrenhoff, H., and Persson, B. N. J., 2018, "Influence of Anisotropic Surface Roughness on Lubricated Rubber Friction: Extended Theory and an Application to Hydraulic Seals," Wear, **410–411**, pp. 43–62.